ALTEX preprint
published October 15, 2020
doi:10.14573/altex.1912131

Research Article

Driver Mutations in Major Lung Cancer Oncogenes can be Analyzed in *Drosophila* Models

Judith Bossen[1#], Karin Uliczka[2,3#], Line Steen[1], Pia Neugebauer[1], Mandy Mong-Quyen Mai[3], Christine Fink[1,4], Frank Stracke[5], Holger Heine[3,4] and Thomas Roeder[1,4]

[1]Kiel University, Zoology, Dept. Molecular Physiology, Kiel, Germany; [2]Research Center Borstel, Priority Area Asthma and Allergy, Division of Invertebrate Models, Borstel, Germany; [3]Research Center Borstel, Priority Area Asthma and Allergy, Division of Innate Immunity, Borstel, Germany; [4]Airway Research Center North (ARCN), German Center for Lung Research (DZL), Germany; [5]Fraunhofer IBMT, Dept. Medical Biotechnology, Sulzbach (Saar), Germany

Abstract

Lung cancer remains the leading cause of cancer-associated mortality. Despite recent promising achievements, the overall prognosis remains very poor. In order to integrate the advantages of adapted, transgenic animal models with a high-throughput procedure on the one hand and compliance with the 3Rs principles on the other hand, we have established and evaluated appropriate *Drosophila* models. To achieve this goal, we ectopically expressed oncogenes representing the most important driver mutations exclusively in the airway system. These oncogenes were either the human oncogenes or the corresponding *Drosophila* orthologs. We have concentrated on two complementary read-out systems, 1) early larval lethality and 2) quantification of concurrently expressed GFP as a proxy for tumor mass. We could show that ectopic expression of *Egfr^{CA}, Ras^{V12}*, *Raf*, *Rolled (MAPK)*, *PI3K92E*, *Alk*, *Akt* and *Arm* can induce early lethality. Thus, they can be used in a straight-forward high-throughput screening approach and can replace mouse models to a considerable extent. Moreover, we could also show that measurement of tumor mass by a concurrently expressed marker (GFP) can be used to detect positive treatment results. Our results show that our *Drosophila* system provides a superb *in vivo* screening system amenable to high-throughput approaches, and thus effectively complements the toolbox for development of novel anti-lung cancer treatments, while complying with the 3R principles.

1 Introduction

Lung cancer is still the leading cause of cancer induced deaths, with annually more than 1 million victims worldwide (Stewart and Wild, 2014). Most lung cancer cases can be assigned as non-small cell lung cancers (NSCLC) that are characterized by extremely poor prognoses (Stewart and Wild, 2014; Travis et al., 2015). The development of NSCLCs most often depends on oncogenic driver mutations found in a relatively small numbers of genes (Luo and Lam, 2013; Ding et al., 2008; Kandoth et al., 2013; Rotow and Bivona, 2017). This oncogenic network comprises receptors and signaling systems that are involved in the control of the proliferative activity of cells. Consequently, growth factor receptors such as the EGFR as well as downstream components of the signaling cascades involved such as Ras, Raf or Erk are major oncogenes that underlie a great number of lung cancer cases. Based on this finding, drugs that specifically target the corresponding gene products or associated signaling pathways are currently used as first- and/or second-line therapies. Although these drugs are tailored to the underlying driver mutations, their effectiveness is currently limited due to development of resistance, inefficient delivery, or toxicity (Kandoth et al., 2013; Rosell et al., 2012). Therefore, novel compounds or combinations of compounds that specifically target these driver mutations or downstream signaling systems are urgently needed as effective therapeutic options. Animal models of these different lung cancer subtypes, especially tailored transgenic mouse models are currently an integral part of corresponding research pipelines. Currently, these mouse models are produced in different ways. Here, both the transfer of oncogenes with e.g. adenoviruses but also the use of inducible expression systems, which limit oncogene expression to the target cells, are of particular interest. In these models, the induction of oncogene expression can simultaneously be time-controlled. These models are complemented by xenografts, in which tumors or metastases are directly transferred into susceptible mouse strains. Common to all these systems is that the tumors have to develop to reach a state comparable to that of a lung cancer patient. This is generally associated with high stress for the affected animals. Due to the development of the tumors, these burdens remain active over a very long period of time (Kwon and Berns, 2013).In order to comply with the 3R principles and to reduce the consumption and harm to these animals, alternative systems are highly appreciated (Olsson et al., 2012). This is especially

[#] authors contributed equally.

Received December 13, 2019; Accepted October 15, 2020;
Epub October 15, 2020; © The Authors, 2021.

ALTEX 38(#), ###-###. doi:10.14573/altex.1912131

Correspondence: Thomas Roeder, PhD
Kiel University, Dept. Molecular Physiology,
Am Botanischen Garten 1-9, 24118 Kiel, Germany
(troeder@zoologie.uni-kiel.de)

relevant as most 3R efforts have focused on toxicological topics although rather than on using alternative transgenic systems based on invertebrate models such as *Drosophila* or *C. elegans* (Kretlow et al., 2010). A highly promising strategy uses tailored invertebrate models to establish large-scale whole-animal screens that enable selection of effective and non-toxic compounds. Only very few animal systems are principally suited for this complex task with *Drosophila* being the most promising one. Recently, a series of different *Drosophila*-based models have been introduced to study chronic lung diseases such as asthma and COPD (chronic obstructive pulmonary disease) (Kallsen et al., 2015; Roeder et al., 2009; Roeder et al., 2012). The inherent logic that underlies the use of *Drosophila* as a model for human lung diseases is the high degree of commonality regarding architecture, physiology, and development (Roeder et al., 2012; Behr, 2010; Ruehle, 1932; Whitten, 1957; Ghabrial et al., 2003; Andrew and Ewald, 2010).

Drosophila has been used as a model for a great variety of different human diseases including various types of cancer. In addition, *Drosophila* has been very successfully used to establish high throughput screening formats that have led to the development of new therapeutic strategies for a number of different cancer types (Bangi et al., 2019; Bangi et al., 2016; Das and Cagan, 2010; Markstein et al., 2014). This type of screening using tailored *Drosophila* methods not only shortcuts research pipelines, it also fully complies with the 3R principles by leading to a reduction in vertebrate animal testing (Kretlow et al., 2010).

Very recently, the first models for human lung cancer based on tailored *Drosophila* have been implemented and used to identify alternative treatment strategies. Levine and Cagan focused on the Ras oncogene and developed a screening system based on ectopic overexpression of constitutively active Ras concurrently with a knockdown of the tumor suppressor PTEN in the airway system to screen for compounds that rescue this lethal phenotype (Levine and Cagan, 2016). A similar approach has been described for constitutively active EGFR, which is also oncogene underlying lung cancer development (Bossen et al., 2019). In both experiments, large scale screening approaches led to the identification of novel combination treatments that might help to fight lung cancer in the future using experimental system that comply with the 3R principles.

Here, we explored the complex oncogene network known to underlie most cases of human lung cancer and exploited whole animal screening approaches that fully comply with the 3R principles. By using tailored *Drosophila* models representing the most important oncogenic driver mutations, a series of personalized lung cancer models could be developed. Ectopic overexpression in the *Drosophila* airway system of most of these oncogenes induced substantial structural changes including epithelial meta- and hyperplasia. We could establish two complementary read out systems, based on either early lethality or tumor mass that proved to be suitable for evaluating the effectiveness of test substances in large scale screening approaches. For both read out indicators we sketch technical concepts for automated measurements. These concepts are both based on *in-situ* contact-less optical technology, hence non-consumptive and repeatable along the larval development. With these *Drosophila* models, novel tools for the development of personalized lung cancer treatments are at hand that fully comply with the 3R principles.

2 Animals, materials and methods

Fly strains and husbandry

Fly stocks were raised on cornmeal agar medium. To ectopically overexpress oncogenes specifically in the airway epithelium, the Gal4/UAS system was used (Brand and Perrimon, 1993). Three different trachea-specific driver lines were utilized to trigger expression of the corresponding genes. The crosses and experiments were carried out at 25 °C, 60-70% humidity and 12h/12h light/dark cycle. The performance of the Gal4/UAS system (btl-Gal4) was improved by using elevated temperatures (30 °C). Temperature sensitive experiments employing temperature sensitive expression control systems (btl-Gal4; Gal80ts) were incubated at 20 °C until hatching and development of the first larval stages and switched to 29 °C for induction of the target gene expression. Transgenic fly strains used for crosses: control line w^{1118} (BDSC_5905), tracheal driver lines for trachea *ppk4*-Gal4 (Wagner et al., 2008; Wagner et al., 2009) and *btl*-Gal4 (Maria Leptin lab, Heidelberg, Germany), *btl-Gal4; tubP-Gal80ts*, *DSRF-Gal4* (Gervais and Casanova, 2011), *UAS-*$Egfr^{CA}$ (BDSC_9533), *UAS-hEGFR-Pvr* (BDSC_58432), *UAS-hEGFR-dEgfr* (BDSC_58415), *UAS-Pvr* (BDSC_8428), *UAS-Apc-RNAi* (BDSC 34869), *UAS-InR* (BDSC_8250), *UAS-htl* (BDSC_5419), *UAS-btl* (BDSC_29045), *UAS-Rl* (BDSC_36270), *UAS-Pi3K92E* (BDSC_8294), *UAS-Akt* (BDSC_8192, 50758), *UAS-Arm* (BDSC_4782), *UAS-Cdk4* (BDSC_6631), *UAS-p53* (BDSC_8422), *UAS-Thor* (BDSC_9147), *UAS-Myc* (BDSC_9675), *UAS-RPTK:Alk* (Ruth Palmer lab, Gothenburg, Sweden), *UAS-Ras* (BDSC_4847), *UAS-Ras(V12)* (Jose C. Pastor-Pareja lab, Beijing, China), *UAS-Raf* (BDSC_2033), *UAS-*$hRAF^{GOF}$ (Markstein lab, Amherst, USA).

Drug treatment

Trametinib (Biomol, Hamburg, Germany), fluvastatin (Enzo, Lörrach, Germany), afatinib (Enzo, Lörrach, Germany), tebipenem pivoxil (Selleckchem, Biozol, Eching, Germany), and cladribine (Selleckchem, Biozol, Eching, Germany) were pipetted directly onto low-melt CM medium (5% (w/v) yeast extract (Becton Dickinson; Heidelberg, Germany), 5% (w/v) sucrose, 8.6% cornmeal, 0.5% (w/v) low-melt agarose, 0.05% (v/v) propionic acid, 0.3% (v/v) methyl-4-hydroxybenzoate) to reach a final concentration of 100 µM. DMSO (0.1%)/ethanol (0.9%) served as a negative control. For trametinib, different concentrations were used. The collected larvae (developed at 20 °C) were deposited on low-melt CM medium and incubated at 29 °C until use (late 3rd instar) for microscopy and GFP quantification.

Measurement of terminal cell branching

3rd instar larvae were deposited in a drop of glycerol on a slide. The larvae were put on 70 °C for 20 s until death and arranged the same way. The pictures of the terminal cells were taken in the GFP channel (10x). To capture all branches of the terminal cell a Z stack projection was performed. The right terminal cell from the 2nd dorsal segment was chosen. The measurement of the GFP pictures occurred in the ImageJ plugin NeuronJ (Meijering et al., 2004) after identical contrast adjustment (1.550 pixels/µm). Statistical analyses were performed with GraphPad Prism7.

Quantification of epithelial thickening and nuclei

The tracheae were dissected from 3rd instar larvae. The tracheae were placed on a drop of a mounting mixture (50% ibidi mounting medium (ibidi, Germany) and 50 % ProLong Diamond Antifade Mountant with DAPI (Thermo Fisher Sci)), set on a slide and covered with coverslip. The tracheal area at the seventh abdominal segment was selected for microscopy. The thickness of the epithelial layer of the dorsal trunk as well as of the primary and secondary branches was measured using the SZX16 fluorescence-stereomicroscope and the cellSens Imaging Software for Life Science Microscopy (Olympus, Germany). Quantification of nuclei was performed at the same tracheal segment (A7). The numbers of nuclei were counted on a 500 µm section of the dorsal trunk, on a 200 µm section of the secondary branch and on a 400 µm section of the secondary branch. For visualization of the nuclei the SZX2-FUV filter and the X-Cite 120 Iris fluorescent lamp were used. Final data were combined of measuring values obtained from at least ten larvae and three measuring points per tracheal area.

GFP quantification

The GFP quantification was performed with 3rd instar larvae. Animals were incubated at 18 °C for egg laying and development of the early larval stages and switched to 29 °C for induction of target gene expression. For the use of 3rd instar larvae, the crossings were incubated at 29 °C for three days before quantification. Treatment with drugs was done for two days before measurement. Three larvae per replicate were collected and homogenized in 200 µl phosphate-buffered saline. The homogenate was directly centrifuged and 100 µl of the supernatant was used for measurement in a black 96-well plate. The fluorescence intensity was measured in a microplate reader (Synergy H1, BioTek Instruments) in an endpoint measurement (excitation: 480 nm, emission: 510 nm). Statistical analyses were performed with GraphPad Prism7. Genotypes: *btl-Gal4*; *tubP-Gal80ts,UAS-GFP>UAS-RasV12 = Ras^{V12}*; *btl-Gal4; tubP-Gal80ts, UAS-GFP* = control.

Measurement of hypoxia sensitivity

3rd instar larvae were collected into a new tube with 20 larvae per replicate. After all larvae were burrowed in the food, they were deposited in a desiccator for hypoxia treatment. Nitrogen was introduced until an O_2 rate of 2-3 % was achieved. The larvae were treated over a period of 25 min. The escaped larvae were counted every 5 min. Statistical analyses were performed with GraphPad Prism7.

3 Results

A complex oncogene network underlies the development of various forms of lung cancer (Ding et al., 2008; Sharma et al., 2007; Siegelin and Borczuk, 2014). We used appropriate *Drosophila* lines to determine whether ectopic activation of these oncogenes can induce cancer-like phenotypes in the *Drosophila* airways and if these phenotypes can be quantified to develop valuable screening systems based on these flies (Fig. 1A). For this purpose, we induced ectopic expression of the corresponding genes exclusively in defined parts of the airway epithelium of *Drosophila* larvae using different airway-specific Gal4 driver lines (Roeder et al., 2009; Kallsen et al., 2015; Wagner et al., 2009) (Fig. 1B-D). We choose three different Gal4 lines that direct expression to different parts of the tracheal system, *btl-Gal4* (Fig. 1B) that induces expression in the entire airway system, *ppk4-Gal4* (Fig. 1C) that targets expression to the entire airway system except the so-called terminal cells and the *DSRF-Gal4* driver (Fig. 1D) that specifically targets these terminal cells. We first used the most specific driver line and induced expression of three different oncogenes *Egfr^{CA}*, *Ras^{V12}*, and *Sem* exclusively in terminal cells (Fig. 2). *Egfr^{CA}* expression in terminal cell showed, in comparison to controls (Fig. 2A, B) only minor effects on the number of terminal branches as well as on their total lengths (Fig. 2E, F). On the other hand, targeted expression of *Ras^{V12}* led to a strong increase in the number of branches as well as in their total length (Fig. 2C, E, F). *Sem* overexpression in these terminal cells induced an intermediate phenotype with significantly higher numbers of branches and higher total length (Fig. 2D-F). The branching phenotype of the terminal cells with *Ras^{V12}* expression was accompanied with enlarged nuclei (Fig. 2G, H). These structural changes had a physiological equivalent, observed as changes of the hypoxia sensitivity. In a classical substrate leaving response, animals experiencing *Ras^{V12}* overexpression in terminal cells showed a higher hypoxia sensitivity compared to the controls (Fig. 2I). Although the observed phenotypical variations were substantial, this approach was not suited to be transformed into a high throughput screening system as the induced changes were neither lethal nor were the changes in the overall fluorescence signal large enough to be accessible to quantification.

All other experiments were performed with driver lines that target expression into all airway cells (*btl-Gal4*) or to all cells except the terminal ones (*ppk4-Gal4*). We tested the entire set of oncogenes available to evaluate if the induced phenotypes are suitable to develop high throughput screening systems. These experimental interventions, which utilized both *Drosophila* orthologs of the corresponding human oncogenes as well as humanized flies carrying the human oncogenes, induced structural changes in the airways in comparison with matching controls (Fig. 3). Here, we show only the effects induced by ectopic overexpression of *egfr* and of *pvr*, driven by the weaker *ppk4-Gal4* line and the stronger *btl-Gal4* line. Controls exhibited a regular appearance of the air conducting lumen (Fig. 3A, white arrowheads), the epithelial layer (Fig. 3A, white arrows), and of the nuclei (Fig. 3A', white arrows). In flies ectopically expressing oncogenes, the most conspicuous change was a substantial thickening of the airway epithelium (Fig. 3B, C, black arrows). Overexpression of *egfr^{CA}* driven by *ppk4* (Fig. 3B) induced this thickening (black arrows) as well as larger and more nuclei (Fig. 3B'', white arrows), indicating an increase in cell number. Using *btl-Gal4* as a driver led to even stronger phenotypes with more disturbed airways (Fig. 3B'). Overexpression of *pvr* driven by *ppk4-Gal4* also led to an increased epithelial thickening (Fig. 3C, black arrows) and structural changes within the air conducting lumen (white arrowhead). The number of nuclei was even higher (Fig. 3C'', white arrow) as observed in *ppk4-Gal4, UAS-egfr^{CA}* animals. Driving *pvr* expression with the stronger *btl-Gal4* driver led to an almost complete breakdown of tracheal structure (Fig. 3C''). To quantify these effects and relate them to the fly's equivalents of lung cancer, we focused on phenotypes directly associated with hyper- or metaplastic changes of the airway epithelium and those ones that may be used as

ALTEX preprint
published October 15, 2020
doi:10.14573/altex.1912131

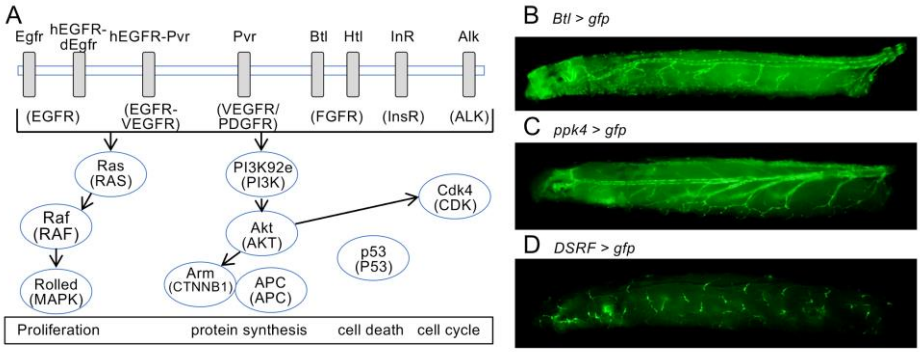

Fig. 1: Targeted expression of oncogenes in different parts of the tracheal system to study their relevance in the airway system
(A) Schematic description of oncogenes used in this study (top of each icon), as well as the corresponding human orthologs (bottom of each icon; graph was modified according to Ding et al. (Ding et al., 2008)). (B-D) Three different Gal4 driver lines were used in this study that target expression to the entire airway system (B, *btl-Gal4*), to the airway system except the terminal cells (C, *ppk4-Gal4*) and to the terminal cells (D, *DSRF-Gal4*).

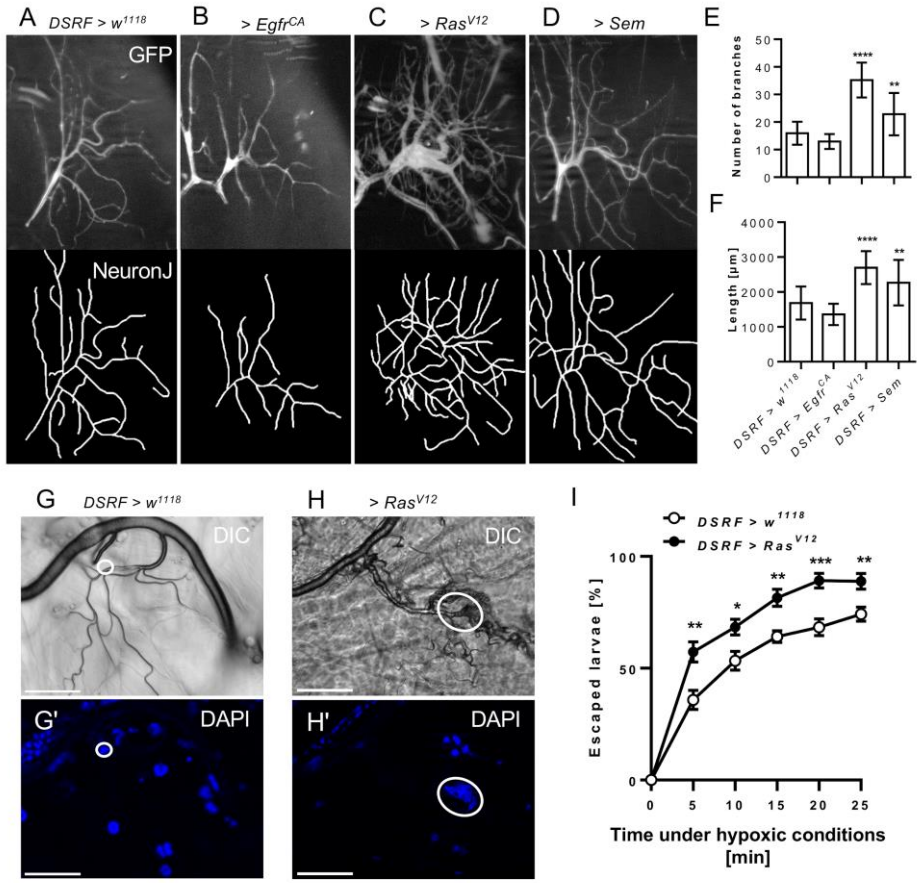

Fig. 2: Targeted expression of oncogenes to the terminal tracheal cells
Overexpression of oncogenes was driven by the *DSRF-Gal4* line. (A-D) GFP expressing terminal cells with overexpression of $Egfr^{CA}$ (B), Ras^{V12} (C) and *Sem* (D) (upper row). The branches of the terminal cells were traced and measured with NeuronJ (lower row). (E, F) Quantification of mean numbers (+SD) of terminal branches, and mean branch lengths (+SD) (n = 14-46). (G, H) Enlarged nuclei of Ras^{V12} expressing animals (H) compared to the control (G). Nuclei were stained with DAPI (G', H'; blue). (I) Hypoxia sensitivity of *DSRF>*Ras^{V12} (n=6) animals compared to the control (n=12) was monitored over a period of 25 min. Scale bar = 50 µm. Statistical significance was evaluated by Mann Whitney test, *, $p < 0.05$, **, $p < 0.01$, ***, $p < 0.001$.

read-outs in high-throughput approaches. Accordingly, we decided to use epithelial thickening as a proxy of metaplastic transformation, and proliferation of airway epithelial cells as a proxy of hyperplasia.

The thickness of an unchallenged epithelial monolayer in the dorsal trunks of L3 larvae was about 2-3 µm (Fig. 4A, C). However, we observed epithelial thicknesses of about 10 µm in *Egfr*-overexpressing dorsal trunks (Fig. 4B, C). Similar epithelial thicknesses were also observed in animals specifically overexpressing *Htl*, *Ras*, and *Raf*. A second group of oncogenes, *Rolled*, *Myc*, *PI3K*, *Akt*, *Thor*, and *InR*, induced epithelial thicknesses in the range of 5 µm, which in all cases differed significantly from the matched controls. By contrast, the increase in epithelial thickness for *Btl* and *Cdk4* was only marginal (Fig. 4C). In primary (Fig. 4D) and secondary branches (Fig. 4E) of the larval tracheal system, we observed very similar changes, but to different extents: the maximal epithelial thickness of primary branches (e.g., in *egfr*-overexpressing flies) was in the range of 5 µm (Fig. 4D), whereas the maximum in secondary branches was about 3–4 µm (Fig. 4E).

As already mentioned, ectopic expression of a variety of oncogenes in the airway system induced by the *ppk4*-Gal4 driver line led to substantial structural changes (Fig. 3, 4). In this system, we observed that ectopic expression of constitutive

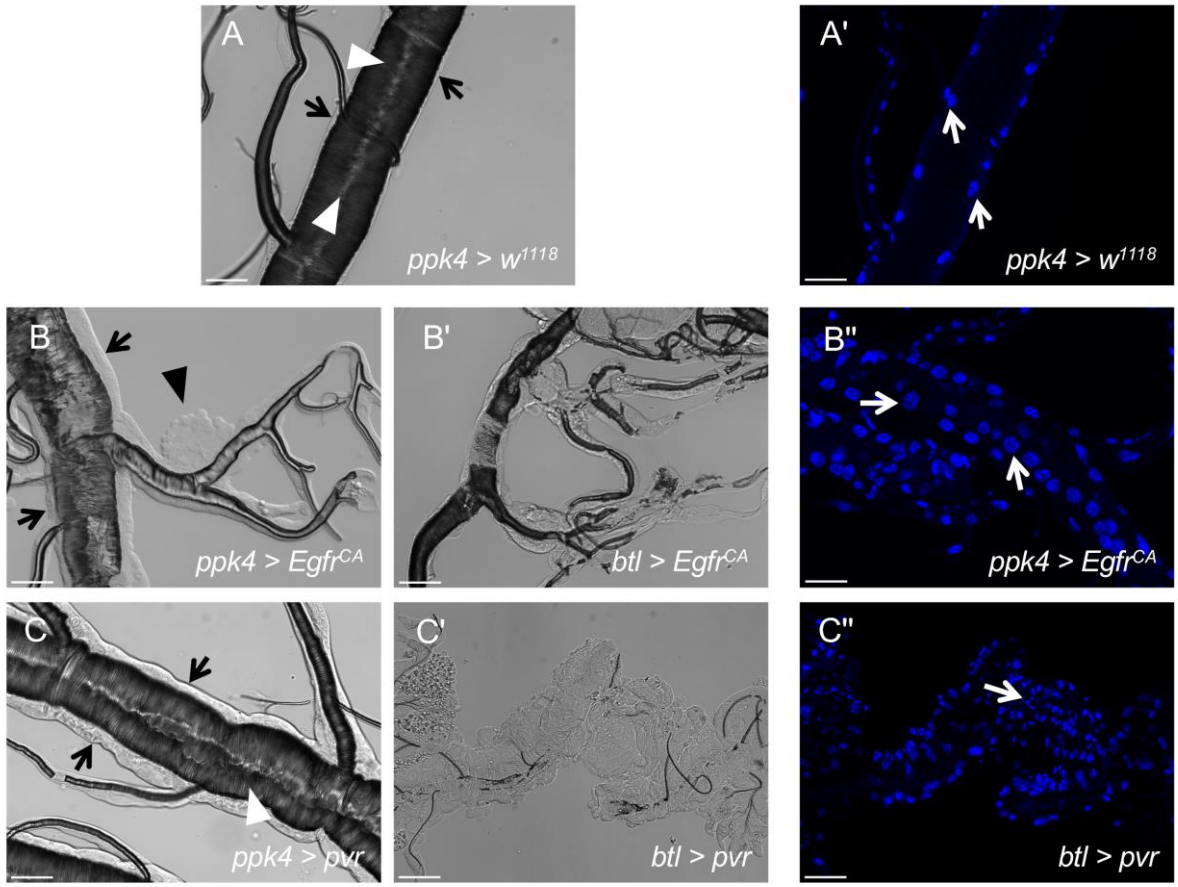

Fig. 3: Ectopic overexpression of oncogenes in the tracheal system induced massive structural changes
Transmitted light images and DAPI staining of the control (A) and trachea with *Egfr^{CA}* (B) and *Pvr* (C) expression. Expression with the moderate *ppk4-Gal4* driver is shown in B and C. Expression with the stronger *btl-Gal4* driver is shown in B' and C'. The epithelial layer is indicated by black arrows (A, B, C). Disordered cell masses are indicated by black arrowheads (B). The air-conducting lumen is indicated by white arrowheads (A, C). Number and size of nuclei are indicated by white arrows, compared to the control (A', B'', C''). Scale bar = 50 µm.

forms of *Drosophila EGFR* (*Egfr^{CA}*) was lethal in larval stages in almost all individuals. Shifting the expression control system towards stronger expression (driven by *btl*-Gal4) caused a greater number of oncogenes to exert lethal effects. Ectopically driven expression of *dEgfr^{CA}*, *hEGFR-dEgfr*, *Pvr*, *Alk*, *Ras*, *Raf*, *Rolled*, *PI3K92E*, *Akt*, and *Arm* led to early lethality, by the early third larval stage at the latest. By contrast, ectopic expression of *Btl*, *InR*, or *Cdk4* had no effect. These results are summarized in Table 1. This oncogene induced lethality is ideally suited as a read-out system, because interventions that rescue this lethality could easily be identified by the occurrence of adult flies in the corresponding test systems. Exactly this approach has been used before for identifying novel combination treatments targeting Ras or EGFR in corresponding *Drosophila* lung cancer models (Levine and Cagan, 2016; Bossen et al., 2019).

Beside using lethality as a read-out for high-throughput approaches, alternative ways to quantify the tumor associated phenotypes are highly appreciated, especially for those cases where early lethality cannot be used as a read-out. Thus, quantifying the GFP-fluorescence that is concurrently expressed together with the oncogene in the airway epithelium would be a suitable alternative (Fig. 5). To test this alternative, *Ras^{V12}* was ectopically expressed together with GFP, enabling to quantify tumor mass. Comparable approaches based on quantification of fluorescence as proxies for tumor mass have been used only occasionally (Willoughby et al., 2013). Therefore, we used *Ras^{V12}* overexpression driven by the heat inducible *btl-Gal4; tubP-Gal80ts* driver that also contained *UAS-GFP* and could observe a substantial increase in the GFP signal of 3rd instar larvae (Fig. 5A') compared with the corresponding controls (Fig. 5A). Quantification of the fluorescence signal using a microplate reader revealed significant differences between controls and those animals showing a *Ras^{V12}* overexpression. Here, application of different compounds (100µM each) rescued the increased fluorescence (trametinib) or it had no or only a very minor affect at this high concentration (fluvastatin, afatinib, tebipenem pivoxil, and cadribine) (Fig. 5B). A more detailed analysis covering a large concentration range was performed with trametinib, the only compound that could rescue the phenotype (Fig. 5C). The experiment revealed a typical s-shaped curve with plateaus at very low and very high concentrations. The IC50 value calculated from these data was 4.9 µM. Fluorescence microscopy showed that the induced tracheal GFP signal was mostly reduced, implying that the tumor mass was reduced accordingly (Fig. 5 D, D').

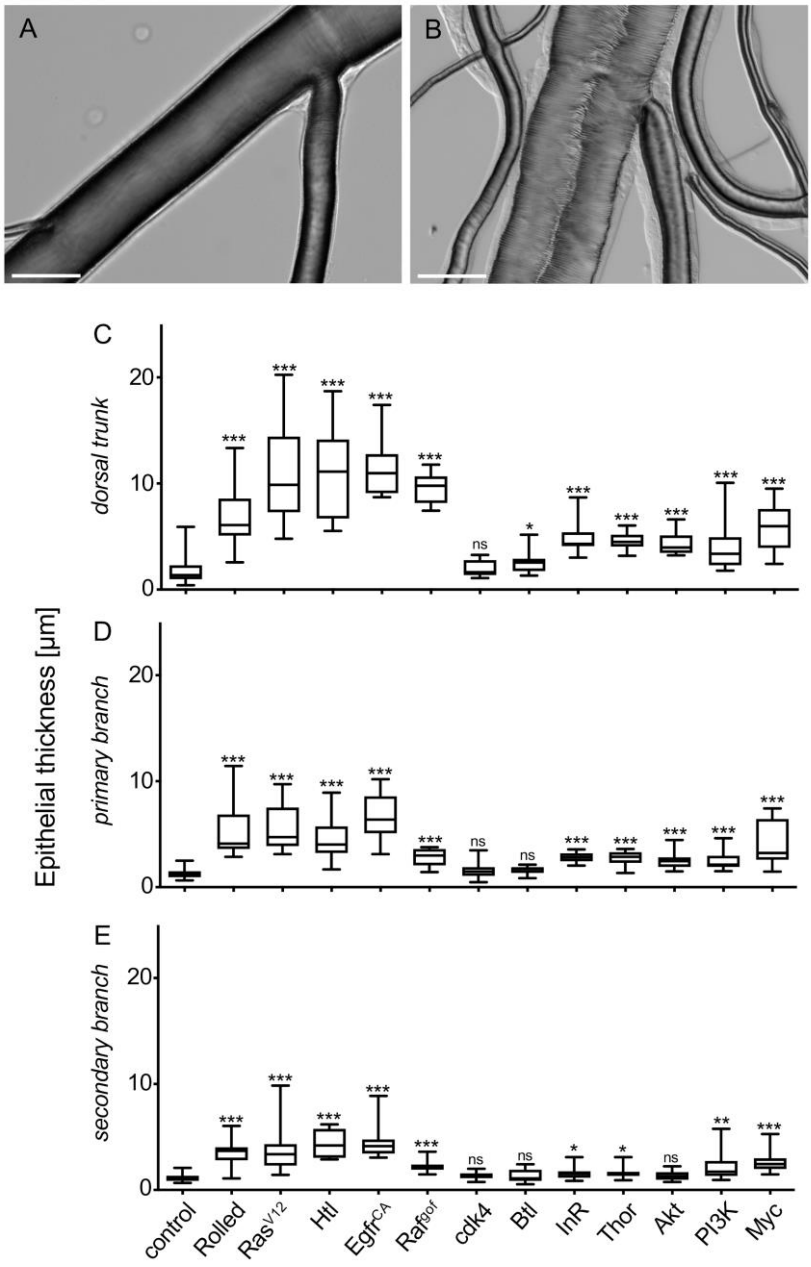

Fig. 4. Ectopic overexpression of oncogenes in the larval airway system induces thickening of the epithelial layer, a proxy for hyperplasia
Epithelial thicknesses differed substantially between tracheae of control flies (*w*^{1118}, A) and those ectopically overexpressing Raf (*ppk4>Raf*^{gof}, B). Scale bar = 50 µm. (C–E) Quantitative evaluation of the effects of ectopic overexpression of various oncogenes. Values obtained from larval dorsal trunks (C), larval primary branches (D), and larval secondary branches (E) are listed. N>20 for each value. Mean values ± S.D. are given. ns means not significantly different from control, *, p<0.05; **, p<0.01; ***, p<0.001.

4 Discussion

In this study, we developed modular *Drosophila* models for a larger number of human lung cancer oncogenes and evaluated if these systems are amenable to high-throughput, whole-animal compound screening approaches. These research efforts should not only provide very useful tools for lung cancer research, they should also be fully consistent with the 3Rs principles and reduce the number of vertebrates used in compound development pipelines. In two recent studies, tailored *Drosophila* systems have been used to identify novel therapeutic strategies to fight specific lung cancer entities based in screening of FDA-approved compound libraries. For this, *Ras*^{V12} overexpression concurrently with downregulation of *Pten* were used to identify a combination of trametinib and fluvastatin as effective strategies to fight *Ras*^{V12} driven lung cancer (Levine and Cagan, 2016). Moreover, targeted overexpression of *Egfr*^{CA} was used to identify combinations of the EGFR agonist afatinib in combination with the STAT inhibitor bazedoxifene to effectively inhibit growth of EGFR initiated tumors (Bossen et al., 2019). Both studies depended on a lethal phenotype that became apparent during early development and that was rescued by the successful pharmacological intervention. The major aim of the current study was to evaluate if other driver mutations can principally also be transformed into high-throughput compatible screening systems. In order to achieve this goal, simple and reliable read-out systems are mandatory that can be performed in microplate formats. These specifications are only fulfilled by two different types of read-outs, the rescue of an otherwise lethal phenotype and the quantification of the tumor mass, which is reduced by successful intervention. Due to its simplicity, the rescue of a lethal phenotype has several advantages, especially as it has a

ALTEX preprint
published October 15, 2020
doi:10.14573/altex.1912131

Tab. 1: Effects of oncogene overexpression on airway hyper- and metaplasia and larval death

***Drosophila* gene (human gene)**	**Tracheal phenotype, larval death (x)**	
	moderate expression *ppk4-Gal4*	strong expression *btl-Gal4*
dEgfr^{CA} (*EGFR*)	+++ (x)	+++ (x)
hEGFR-dEgfr	-	++ (x)
hEGFR-Pvr	-	+
Btl (*FGFR*)	-	-
Htl (FGFR)	++	nd
Pvr (*VEGFR/PDGFR*)	++	+++ (x)
InR (*InsR*)	-	-
Alk (*ALK*)	+	+++ (x)
Ras^{V12} (*RAS*)	+	+++ (x)
hRaf^{gof} (*RAF*)	+	+++ (x)
Rl (*MAPK*)	+	+++ (x)
PI3K92E (*PI3K*)	+	+++ (x)
Akt (*AKT*)	-	+++ (x)
Arm (*CTNNB1*)	+	+++ (x)
Apc (*APC*)	+	+
Cdk4 (*CDK*)	-	-
Thor (THOR)	+	nd
Myc (MYC)	+	nd
P53 (*TP53*)	+	+

The phenotype induced by ectopic overexpression of the corresponding oncogene is given. Oncogenes of human origin are underlined. +, visible phenotype, ++, strong phenotype, +++ very strong phenotype, X, lethality, -, no effect; nd, not determined.

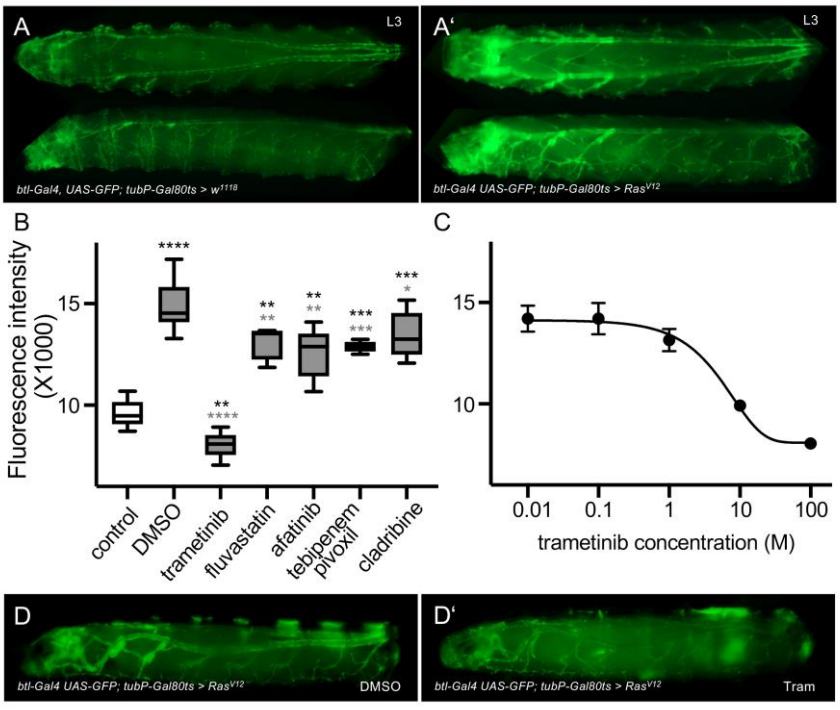

Fig. 5: Quantification of GFP expression in the airway system as a proxy of tumor mass
(A) GFP expressing 3rd instar larvae after three days of induction are shown in dorsal and lateral view. (B) Measured fluorescence intensity of animals treated with different drugs (concentration: 100 µM each). DMSO treated *Ras^{V12}* animals and animals without *Ras^{V12}* expression served as control (n=4-15, whiskers show min and max). (C) Quantification of fluorescence intensity in *Ras^{V12}* overexpressing animals treated with different concentrations of trametinib shown in a dose-response curve (n=6-9, means and SEM are shown). (D) *Ras^{V12}* expressing animals treated with trametinib (100 µM) (D') have less GFP expression compared to untreated animals (D). Statistical significance was tested by Mann-Whitney test, ****, p<0.0001; ***, p<0.001; **, p<0.01; *, p<0.05.

digital design allowing to distinguish successful and failed interventions with low instrumental input. For automated recognition of living larvae besides dead ones, we focus on larvae motility. Instead of applying video microscopy and analysis, we will evaluate a diffraction-based optical technology ("Speckle" sensing) for this task. The technology was developed for the determination of beating frequencies in freely floating cardiomyocyte spheroids. To this end, the illumination will be altered to a multiplex beam pattern filling the well's cross section. While cardiomyocyte signals are a sequence of almost identical peaks that may be easily analyzed, signals from larvae motions will be irregular. Hence the signal analysis will make use of noise analysis techniques in order to quantify the number of vital larvae per well.

On the other hand, quantifying tumor mass, in the current study via co-expressed GFP allows to quantify effects beyond the simple yes or no experimental design, but it requires more sophisticated instrumental efforts. These strategies are in line with other successful high-throughput-screening (HTS) assays for specific cancer subtypes based on *in vivo* analysis of tailored *Drosophila* strains (Levinson and Cagan, 2016; Das and Cagan, 2010; Willoughby et al., 2013; Markstein et al., 2014). Broadly speaking, studies that utilize *in vivo Drosophila* HTS assays take advantage of the long history of using *Drosophila* to advance our general understanding of cancer biology (Gonzalez, 2013; Gateff, 1978; Harrison et al., 1995). The recent finding that Ras^{V12} and $EGFR^{CA}$ overexpression are well suited to develop high-throughput screening systems converted the general assumption that diseases like lung cancer could not be modeled in *Drosophila* completely (Levine and Cagan, 2016; Bossen et al., 2019). The usefulness of this type of *Drosophila* cancer models was further supported by the development of personalized screening platforms based on transgenic *Drosophila* that can be used for different cancer entities (Bangi et al., 2016, 2019). In this study, we showed that most components of the oncogenic network underlying the vast majority of adenocarcinomas (Ding et al., 2008; Kandoth et al., 2013; Paez et al., 2004; Travis et al., 2015) are able to induce lung cancer-like phenotypes in *Drosophila*. These phenotypes, primarily hyper- and metaplasia of airway epithelial cells, are not exact copies of the histological features of human lung cancer, but they are the closest equivalent in the fly, and give rise to quantifiable and cancer-associated phenotypes. The observation that the majority of the known oncogenes (Tab. 1) could induce structural changes related to hyper- and metaplasia in the fly's airway epithelium implies that the model that has been proposed for mutations in *EGFR* or *Ras* could also be adapted to other oncogenes, raising the possibility of generating panels of personalized fly models for human lung cancers with different driver mutations. Beside the ectopic overexpression of constitutively active *Egfr* and Ras^{V12}, ectopic overexpression of *Raf*, *Rolled* (MAPK), *PI3K92E* (PI3K), *Akt* (AKT), *Alk* and *Armadillo* (CTNNB1) also induced lethal phenotypes making them ideally suited to be developed into personalized high-throughput screening systems for the corresponding lung cancer subtypes (Tab. 1). The inherent features of the screening approach that is based on long-term treatment with the compounds of interest encompassing the entire development of the animals, only those candidate substances are assessed as positive that do not interfere with normal physiology or development. The pharmacological data that can be obtained with this system are certainly in ranges that are also used in therapy. In the case of trametinib, for which we were able to determine an IC50 of 4.9µM, there is little clinical data. Trametinib is used as a combination therapy with dabrafenib in a variety of tumor diseases (Adachi et al., 2020). Taking into account the long residence time of trametinib, the concentration of trametinib is approximately 0.2µmol/kg body weight, which could correspond to a concentration in body fluids of approximately 0.4µmol/l. If we also take into account that the IC50 value determined by us refers to the concentration in food, we are dealing with very similar concentration ranges. The same can be said about the comparison with the studies of Levine and Cagan (Levine and Cagan, 2016). Here, 0.5 µM trametinib was used, but in combination with a statin, which showed synergistic effects with a factor of 5-8. Also there, we are thus in very comparable concentration ranges.

To further expand the use of *Drosophila* as a screening tool for the identification of novel treatment strategies for those oncogenes that did not induce early larval lethality in *Drosophila*, alternative read-outs would be highly appreciated. Therefore, alternative strategies that employ signals from concurrently with the oncogenes expressed markers such as luciferase or GFP are principally suitable as they give a proxy for tumor mass (Markstein et al., 2014). Thus, we aimed to test this approach using concurrently expressed GFP. Based on our findings, we could show that this strategy can be used to quantify increased cell mass and therewith higher GFP expression in the trachea only using microplate-based fluorescence analyses of whole animals, therewith further widening the group of oncogenes that can be used for personalized *Drosophila* screening approaches. In order to transfer the tumor mass quantification read out into an *in-situ* measurement ready for non-consumptive and automated operation requires fluorescence acquisition of intact larvae in the plate wells. One approach to this end was already described (Willoughby et al., 2013): The larvae are immersed in aqueous sucrose solution in order to take care for their proper position and orientation. Then fluorescence images are taken and transformed into one bit (black/white) image using a constant threshold brightness. The number of white pixels is then used as the measure of tumor mass. In order to have a repeatable read out, a fluorescence quantification technique that works without liquid immersion on any possible position and orientation of the larvae in the well is preferable. Such a technique requires transparent feeding media and very high fluorescence collection efficiency as in an integrating sphere. No imaging nor image analysis is needed using this type of integrating techniques.

Based on the finding of this study and of the two recent publications employing the first *Drosophila* lung cancer models (Bossen et al., 2019; Levine and Cagan, 2016), a panel of personalized *Drosophila* models amenable to high-throughput screening approaches can be installed that act as shortcuts for the development of novel therapeutic strategies. In order to be able to use personalized models of lung tumors, these must essentially be available, as patients do not have enough time. However, this is perfectly feasible with the *Drosophila* systems. For this, the corresponding oncogene overexpressing flies (without the corresponding drivers) should already be available in a number of important combinations. The keeping of 100 or more oncogene combinations can be easily done. These would then only have to be crossed with the respective inducible drivers and the corresponding experiments could be completed within 2 weeks. Expanding the application of the 3R principles beyond the field of toxicology holds the potential to substantially reduce the requirements of vertebrates as animal test systems (Blakemore et al., 2012; Graham and Prescott, 2015). Although these *Drosophila* systems offer a greater number of impressive advantages, limitations of these systems should not be overlooked. Only the tumor itself can be analyzed in the most accurate way. The tumor environment, however, remains the same as it is found in *Drosophila*. For this reason, it is always necessary to carry out experiments in e.g. mouse models for those very few compounds that have been identified and characterized in

depth in order to independently verify the results. Nevertheless, it should be noted that the use of suitable *Drosophila* models will lead to a massive reduction of the required mouse experiments.

In summary, here we have described a large number of personalized *Drosophila* lung cancer models that provide us with novel tools to identify suitable treatment strategies for lung adenocarcinomas. This valuable screening approach opens a new direction for cancer research, namely, the identification of new anticancer drugs using high-throughput whole-animal screens.

References

Adachi, Y., Yanagimura, N., Suzuki, C. et al. (2020). Reduced doses of dabrafenib and trametinib combination therapy for braf v600e-mutant non-small cell lung cancer prevent rhabdomyolysis and maintain tumor shrinkage: A case report. *BMC Cancer 20*, 156. doi:10.1186/s12885-020-6626-9

Andrew, D. J. and Ewald, A. J. (2010). Morphogenesis of epithelial tubes: Insights into tube formation, elongation, and elaboration. *Dev Biol 341*, 34-55. doi:10.1016/j.ydbio.2009.09.024

Bangi, E., Murgia, C., Teague, A. G. et al. (2016). Functional exploration of colorectal cancer genomes using drosophila. *Nat Commun 7*, 13615. doi:10.1038/ncomms13615

Bangi, E., Ang, C., Smibert, P. et al. (2019). A personalized platform identifies trametinib plus zoledronate for a patient with kras-mutant metastatic colorectal cancer. *Sci Adv 5*, eaav6528. doi:10.1126/sciadv.aav6528

Behr, M. (2010). Molecular aspects of respiratory and vascular tube development. *Respir Physiol Neurobiol 173 Suppl*, S33-36. doi:10.1016/j.resp.2010.04.011

Blakemore, C., MaCarthur Clark, J., Nevalainen, T. et al. (2012). Implementing the 3rs in neuroscience research: A reasoned approach. *Neuron 75*, 948-950. doi:10.1016/j.neuron.2012.09.001

Bossen, J., Uliczka, K., Steen, L. et al. (2019). An egfr-induced drosophila lung tumor model identifies alternative combination treatments. *Mol Cancer Ther* doi:10.1158/1535-7163.MCT-19-0168

Brand, A. H. and Perrimon, N. (1993). Targeted gene expression as a means of altering cell fates and generating dominant phenotypes. *Development 118*, 401-415.

Das, T. and Cagan, R. (2010). Drosophila as a novel therapeutic discovery tool for thyroid cancer. *Thyroid 20*, 689-695. doi:10.1089/thy.2010.1637

Ding, L., Getz, G., Wheeler, D. A. et al. (2008). Somatic mutations affect key pathways in lung adenocarcinoma. *Nature 455*, 1069-1075. doi:10.1038/nature07423

Gateff, E. (1978). Malignant neoplasms of genetic origin in drosophila melanogaster. *Science 200*, 1448-1459. doi:10.1126/science.96525

Gervais, L. and Casanova, J. (2011). The drosophila homologue of srf acts as a boosting mechanism to sustain fgf-induced terminal branching in the tracheal system. *Development 138*, 1269-1274. doi:10.1242/dev.059188

Ghabrial, A., Luschnig, S., Metzstein, M. M. et al. (2003). Branching morphogenesis of the drosophila tracheal system. *Annu Rev Cell Dev Biol 19*, 623-647. doi:10.1146/annurev.cellbio.19.031403.160043

Gonzalez, C. (2013). Drosophila melanogaster: A model and a tool to investigate malignancy and identify new therapeutics. *Nat Rev Cancer 13*, 172-183. doi:10.1038/nrc3461

Graham, M. L. and Prescott, M. J. (2015). The multifactorial role of the 3rs in shifting the harm-benefit analysis in animal models of disease. *Eur J Pharmacol 759*, 19-29. doi:10.1016/j.ejphar.2015.03.040

Harrison, D. A., Binari, R., Nahreini, T. S. et al. (1995). Activation of a drosophila janus kinase (jak) causes hematopoietic neoplasia and developmental defects. *EMBO J 14*, 2857-2865. doi:10.1002/j.1460-2075.1995.tb07285.x

Kallsen, K., Zehethofer, N., Abdelsadik, A. et al. (2015). Ormdl deregulation increases stress responses and modulates repair pathways in drosophila airways. *J Allergy Clin Immunol 136*, 1105-1108. doi:10.1016/j.jaci.2015.04.009

Kandoth, C., McLellan, M. D., Vandin, F. et al. (2013). Mutational landscape and significance across 12 major cancer types. *Nature 502*, 333-339. doi:10.1038/nature12634

Kretlow, A., Butzke, D., Goetz, M. E. et al. (2010). Implementation and enforcement of the 3rs principle in the field of transgenic animals used for scientific purposes. Report and recommendations of the bfr expert workshop, may 18-20, 2009, berlin, germany. *ALTEX 27*, 117-134. doi:10.14573/altex.2010.2.117

Kwon, M. C. and Berns, A. (2013). Mouse models for lung cancer. *Mol Oncol 7*, 165-177. doi:10.1016/j.molonc.2013.02.010

Levine, B. D. and Cagan, R. L. (2016). Drosophila lung cancer models identify trametinib plus statin as candidate therapeutic. *Cell Rep 14*, 1477-1487. doi:10.1016/j.celrep.2015.12.105

Levinson, S. and Cagan, R. L. (2016). Drosophila cancer models identify functional differences between ret fusions. *Cell Rep 16*, 3052-3061. doi:10.1016/j.celrep.2016.08.019

Luo, S. Y. and Lam, D. C. (2013). Oncogenic driver mutations in lung cancer. *Transl Respir Med 1*, 6. doi:10.1186/2213-0802-1-6

Markstein, M., Dettorre, S., Cho, J. et al. (2014). Systematic screen of chemotherapeutics in drosophila stem cell tumors. *Proc Natl Acad Sci U S A 111*, 4530-4535. doi:10.1073/pnas.1401160111

Meijering, E., Jacob, M., Sarria, J.-C. F., et al. (2004). Design and Validation of a Tool for Neurite Tracing and Analysis in Fluorescence Microscopy Images. *Cytometry Part A 58*, 167-176. doi:10.1002/cyto.a.20022

Olsson, I. A. S., Franco, N. H., Weary, D. M. et al. (2012). The 3rs principle–mind the ethical gap. ALTEX Proceedings: Proceedings of the 8 th World Congress on Alternatives and Animal Use in the Life Sciences, Montreal. *Johns Hopkins University Press* 333-336.

Paez, J. G., Janne, P. A., Lee, J. C. et al. (2004). Egfr mutations in lung cancer: Correlation with clinical response to gefitinib therapy. *Science 304*, 1497-1500. doi:10.1126/science.1099314

Roeder, T., Isermann, K. and Kabesch, M. (2009). Drosophila in asthma research. *Am J Respir Crit Care Med 179*, 979-983. doi:10.1164/rccm.200811-1777PP

Roeder, T., Isermann, K., Kallsen, K. et al. (2012). A drosophila asthma model - what the fly tells us about inflammatory diseases of the lung. *Adv Exp Med Biol 710*, 37-47. doi:10.1007/978-1-4419-5638-5_5

Rosell, R., Carcereny, E., Gervais, R. et al. (2012). Erlotinib versus standard chemotherapy as first-line treatment for european patients with advanced egfr mutation-positive non-small-cell lung cancer (eurtac): A multicentre, open-label, randomised phase 3 trial. *Lancet Oncol 13*, 239-246. doi:10.1016/S1470-2045(11)70393-X

Rotow, J. and Bivona, T. G. (2017). Understanding and targeting resistance mechanisms in nsclc. *Nat Rev Cancer 17*, 637-658. doi:10.1038/nrc.2017.84

Ruehle, H. (1932). Das larvale tracheensystem von drosophila melanogaster meigen und seine variabilität. *Zeitschrift für wissenschaftliche Zoologie 141*, 159-245.

Sharma, S. V., Bell, D. W., Settleman, J. et al. (2007). Epidermal growth factor receptor mutations in lung cancer. *Nat Rev Cancer 7*, 169-181. doi:10.1038/nrc2088

Siegelin, M. D. and Borczuk, A. C. (2014). Epidermal growth factor receptor mutations in lung adenocarcinoma. *Lab Invest 94*, 129-137. doi:10.1038/labinvest.2013.147

Stewart, B. W. and Wild, C. P. *World cancer report 2014*. International agency for research on cancer. Vol. WHO Press.

Travis, W. D., Brambilla, E., Nicholson, A. G. et al. (2015). The 2015 world health organization classification of lung tumors: Impact of genetic, clinical and radiologic advances since the 2004 classification. *J Thorac Oncol 10*, 1243-1260. doi:10.1097/JTO.0000000000000630

Wagner, C., Isermann, K., Fehrenbach, H. et al. (2008). Molecular architecture of the fruit fly's airway epithelial immune system. *BMC genomics 9*, 446. doi:10.1186/1471-2164-9-446

Wagner, C., Isermann, K. and Roeder, T. (2009). Infection induces a survival program and local remodeling in the airway epithelium of the fly. *FASEB J 23*, 2045-2054. doi:10.1096/fj.08-114223

Whitten, J. (1957). The post-embryonic development of the tracheal system in drosophila melanogaster. *Q. J. Microsc. Sci. 98*,

Willoughby, L. F., Schlosser, T., Manning, S. A. et al. (2013). An in vivo large-scale chemical screening platform using drosophila for anti-cancer drug discovery. *Dis Model Mech 6*, 521-529. doi:10.1242/dmm.009985

Conflict of interest

The authors declare no conflict of interest.

Acknowledgments

The work was funded by grants of the BMBF as part of program “Alternativen zum Tierversuch” (FKZ 031L0110A - DroLuCa) and the Else-Kröner-Fresenius-Stiftung. Moreover, we would like to thank Britta Laubenstein and Christiane Sandberg for excellent technical assistance.